Detection and Classification of Double Line to Ground Faults in a 138 kV Six Phase Transmission Line Using Hilbert Huang Transform

Gaurav Kapoor

Department of Electrical Engineering, Modi Institute of Technology, Kota, India
gaurav.kapoor019@gmail.com

Abstract – *This paper presents a single ended Hilbert Huang transform (HHT) based double line to ground fault detection and faulty phase identification technique for a six phase transmission line. HHT is employed to extort the information of transients from the measured six phase current signals. The HHT coefficients of the six phase current signals are used to detect the fault and identify the faulty phase. The simulation studies are carried out using MATLAB. The performance of the proposed technique is tested for different fault types, fault resistances, fault inception time, fault locations, and ground resistances with satisfactory test results.*

Keywords: *fault detection, faulty phase identification, Hilbert Huang transform, six phase transmission line protection.*

I. Introduction

The modern era has observed a raise in the requirement of electricity and to support the increasing need of electricity, the power transfer capability of active power transmission network should be boosted. Higher phase order (six phase) transmission lines have been proposed as a prospective alternative which have the possibilities to transfer the large quantity of electrical power with no chief alteration in the current structure of power transmission system.

Due to the connections of large number of conductors, the probability of event of faults on six phase transmission line is more. Thus, it is also important to develop a satisfactory protection technique, which would decide the faulty phase to drop off the restoration period and hence improve the stability of the power transmission system. The larger number of feasible fault combinations in six phase transmission line makes the difficulty of detecting/classifying the faults very complicated. A number of outstanding works have been stated in the literatures on the topics associated to the protection and economics of six phase transmission lines. Some noteworthy investigations are discussed in detail in this section. Reference [1] used the wavelet transform to design the fault detection and classification tool for the boundary protection of six phase transmission line. The effectiveness of the fault detection and classification algorithm is validated through investigating the effect of variation in different fault parameters such as fault type,

fault resistance, fault inception time, ground resistance and fault location. In [2], a phase to phase fault detection technique, using wavelet transform, has been proposed for the series capacitor compensated six phase transmission line protection. They have analyzed the effect of variation in fault type, fault inception time, fault resistance, ground resistance and fault location. A somewhat different mathematical morphology based fault detection and faulty phase identification technique has been proposed in [3] for the boundary protection of six phase transmission line. The norm of wavelet transform has been used in [4] for fault detection and faulty phase identification in series capacitor compensated six phase transmission line. The study reported in [5], shows that a fault detection and classification technique that employs wavelet transform has been developed for the protection of 400 kV extra high voltage transmission line. The effectiveness of the technique is authenticated through investigating the effect of variation in different fault parameters such as fault location, fault resistance, fault inception angle and fault type. In the study described in [6], Fourier transform and support vector machine (SVM) based asymmetrical and symmetrical faults classification method has been investigated for the protection of a 400 kV series compensated transmission line during power swing situations. To evaluate the performance of the fault classification method, the authors have analyzed the effect of variation in fault type, fault inception time, fault resistance, degree of series compensation, power flow angle and fault location. Reference [7] proposed an

effective fault detection and classification scheme using functional analysis and computational intelligence for the protection of a 230 kV, 200 km long transmission line. Authors have simulated different types of symmetrical, unsymmetrical and open conductor faults with the effect of variation in fault type, fault inception angle, fault resistance, load angle and fault location. A combination of Fourier transform (FT) and decision tree (DT) has been used in [8] to analyze the superimposed currents, and an effectual approach to fast and accurate fault detection and classification has been achieved. Authors have discussed the effect of variation in fault resistance, fault location, fault type, fault inception angle and degree of series compensation. Reference [9] described the artificial neural network (ANN) and phasor data (PD) based technique in detail and pointed out that a combination of ANN and PD is an excellent tool for islanding detection in smart grids. The effectiveness of the islanding detection and classification technique is authenticated through investigating the effect of variation in fault type, fault resistance, generator and load ratings variations. In [10], authors used travelling wave theory to design the fault detection and classification tool for the protection of voltage source converter (VSC) based HVDC grids. Authors performed fault analysis on VSC-HVDC grid test system in phase and modal domains. Reference [11] proposed an effective back-up protection technique for the protection of three terminals double circuit transmission lines. The usefulness of the fault detection, classification and location technique is validated through investigating the consequence of variation in different fault parameters such as fault type, fault resistance, fault inception angle and fault location. The study reported in [12] demonstrates that a hybrid scheme that combines Sparse transform (S-transform) and FFNN (fast forward neural network) has been developed for the protection of distribution grids. To assess the performance of the proposed hybrid scheme, the authors have analyzed the effect of variation in fault type, fault inception angle, fault resistance and fault location. In [13], a fault protection technique using a decision tree (DT) based fault detector, classifier and locator has been proposed for the protection of a 400 kV, two terminals, 200 km long double circuit transmission line. The authors have analyzed the effect of variation in fault type, fault inception angle, fault resistance and fault location. A combination of Hilbert Huang transform (HHT) and wavelet packet transform (WPT) is used in [14] for small current grounding faults location on a 110 kV transmission line. However, the work was only restricted to the grounding faults and other types of faults

were not considered. Authors have analyzed the effect of variation in fault resistance, fault inception angle, fault location and fault type. In [15], a protection technique using discrete wavelet transform has been proposed for the protection of series capacitor compensated twelve phase transmission line.

Recently, protection of poly-phase power transmission lines has engaged much consideration from researchers and a very less research has been made on six phase transmission line protection. Current research has been focused on the protection of six phase power transmission line against a variety of double line to ground faults using Hilbert Huang transform. No such type of work has been published so far to the best of the awareness of the author. Test results show that the proposed method well detects and classifies the double line to ground faults and the reliability of the proposed technique is not affected by variation in fault parameters.

This paper is structured as follows: schematic of six phase transmission line is described in Section II. Brief introduction of Hilbert Huang transform and the development of proposed fault detection scheme based on Hilbert Huang transform are presented in Section III. Section IV is devoted to the discussion of test results. Section V concludes the paper.

II.   Six Phase Transmission Line Specifications

MATLAB/ Simscape power system tool box is employed to assess the proposed double line to ground fault detection technique. The simulated test system is a typical 138 kV, six phase transmission line of Allegheny power system located at Springdale McCalmont which is depicted in Fig. 1. As can be seen from Fig. 1, there are two 138 kV voltage sources, both connected to a 68 km long six phase transmission line. The six phase transmission line is bifurcated into two sections. The length of each section is 34 km. As can be seen from Fig. 1, two loads of 300 MW and 150 MVAr are connected at the second terminal i.e. at bus-2 of six phase transmission line. As depicted in Fig. 1, the relay is connected at bus-1 to detect the faults on the whole length of six phase transmission line.

The six phase pre fault current (I_A, I_B, I_C, I_D, I_E, I_F) and voltage (V_A, V_B, V_C, V_D, V_E, V_F) waveforms of corresponding phases are shown in Fig. 2. Fig. 3 depicts the Hilbert Huang coefficients of six phase current during no-fault. Table I reports the response of the proposed technique during no-fault situation.
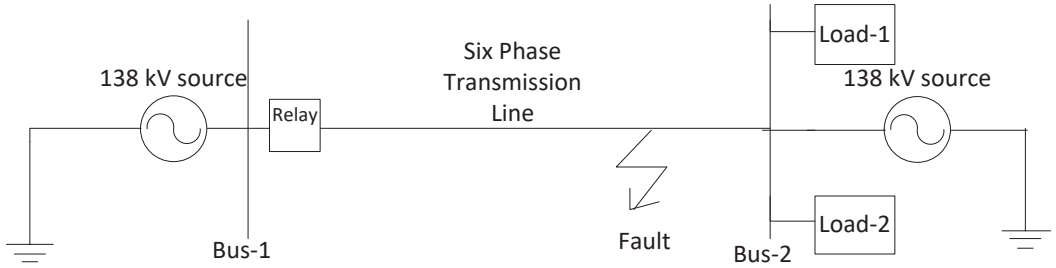
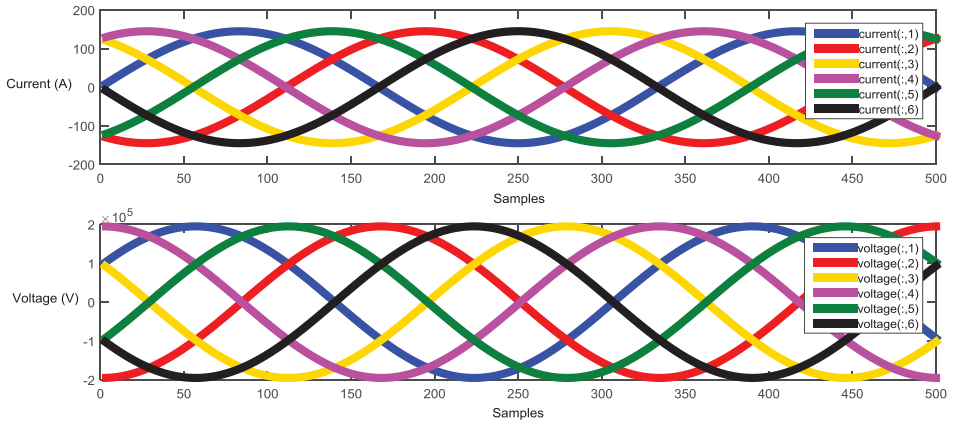Fig. 1. Single line diagram of six phase power system

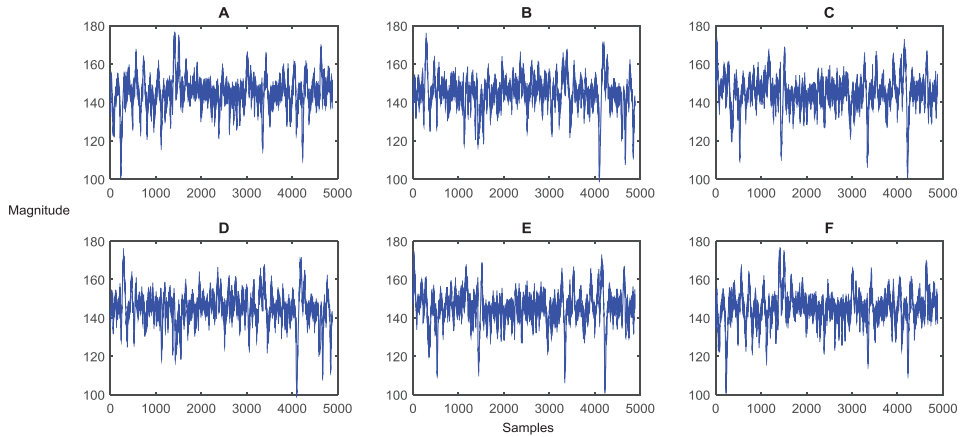Fig. 2. Six phase current and voltage waveforms during no-fault

Fig. 3. Hilbert Huang transform coefficients of six phase current during no-fault

TABLE I
TEST RESULT FOR NO FAULT

Phase	Hilbert Huang Transform Coefficients
A	174.2505
B	173.6513
C	171.7558
D	173.6695
E	171.9691
F	174.2560

III. Hilbert Huang Transform and Proposed Fault Detection Technique

Hilbert-Huang Transform (HHT) is [14] utilized for the processing of non-stationary and nonlinear signals such as, power signals. The Hilbert transform is used to localize a signal in both time and frequency, through a theory called the instantaneous frequency. The instantaneous magnitude is the magnitude of the complex Hilbert transform. The HHT is shown to be an effective technique for detecting faults due to its ability of estimating the instants at which the frequency of signal changes immediately.

The Hilbert transform for a test signal f (t) is defined as given in equation (1) below [14]:

$$H\{f(t)\} = -\frac{1}{\pi} \int_{-\infty}^{\infty} f(\tau) \frac{d\tau}{\tau - t} = -\frac{1}{\pi t} * f(t)$$

(1)

Hilbert transform can be defined as the convolution between f(t) and $-1/\pi t$.

This equation defines an inappropriate integral, because for $t = \tau$ the integral has an exceptionality. So the integral is calculated symmetrically to avoid this difficulty.

$$\int_{-\infty}^{\infty} \frac{g(\tau)}{t - \tau} d\tau = \lim_{e \to 0} \left[\int_{-\infty}^{t-e} \frac{g(\tau)}{t - \tau} d\tau + \int_{t+e}^{\infty} \frac{g(\tau)}{t - \tau} d\tau \right]$$

(2)

Inverse Hilbert transform can be deliberated by equation given below, where g' (t) and g (t) are part of pair transform of Hilbert [14]

$$g(t) = -\frac{1}{\pi} \int_{-\infty}^{\infty} \frac{g'(t)}{t - \tau} * d\tau$$

(3)

From the definition of Hilbert Transform it is observed that g' (t) can be understood as the convolution of g (t) with the signal $-1/\pi t$.

$$g'(t) = g(t) * \frac{1}{\pi t}$$

(4)

Fig. 4 shows the flow chart of the proposed fault detection and faulty phase identification technique with the following steps:

Step-1: Six phase currents are measured through the current measurement units connected at bus-1.

Step-2: Hilbert Huang transform is applied to calculate the Hilbert Huang coefficients of each phase current signal.

Step-3: If the magnitude of Hilbert Huang coefficients of the faulted phase is greater than the magnitude of Hilbert Huang coefficients of un-faulted phase, then fault detection and faulty phase identification else no fault detection, go to step 1.
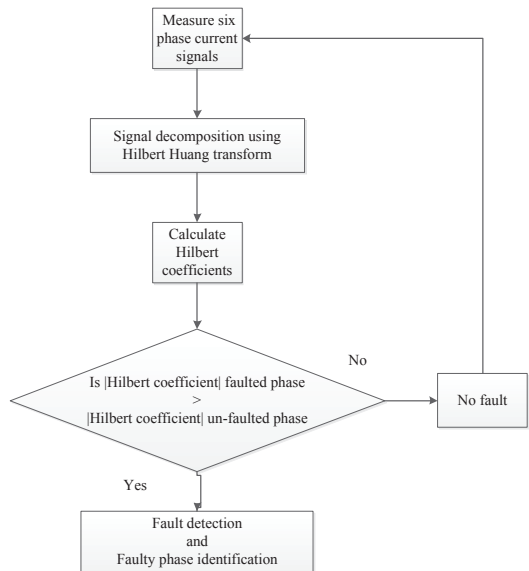

Fig. 4. Representation of proposed fault detection and faulty phase identification technique

IV. Test Results and Discussions

To validate the efficacy of the proposed fault detection/ classification technique, test studies have been approved for numerous types of double line to ground faults. The effect of variation in fault type (F_t), fault location (F_l), fault inception time (FIT), fault resistance

(R_f), and ground resistance (R_g) has been examined. The simulation results are discussed in the successive subsections.

A. *Performance in Case of ABG Fault: Case-I*

The effectiveness of the proposed fault detection technique has been evaluated for ABG double line to ground fault when ABG fault is simulated at 5 km away from the relaying point at fault inception time of 0.05 seconds with R_f= 5 Ω and R_g = 10 Ω. Fig. 5 demonstrates the waveform of six phase current when the six phase transmission line is subjected to ABG fault at 5 km away from the relay location at FIT = 0.05 seconds. The process of feature extraction using Hilbert Huang

transform for six phase current during ABG fault is depicted in Fig. 6. Fig. 6 depicts the Hilbert Huang transform coefficients of six phase current during ABG fault. As observed from Fig. 6, the magnitudes of Hilbert Huang coefficients of phase-'A' and 'B' are greater than the magnitudes of Hilbert Huang coefficients of other phases. Table II depicts the response of proposed fault detection and classification technique for ABG fault. From the simulation results as shown in Table II, it is clear that the magnitudes of Hilbert Huang coefficients of the faulted phases are greater than the magnitudes of Hilbert Huang coefficients of the healthy phases. Therefore, it is clear from Table II that the ABG fault is correctly detected by the proposed technique.
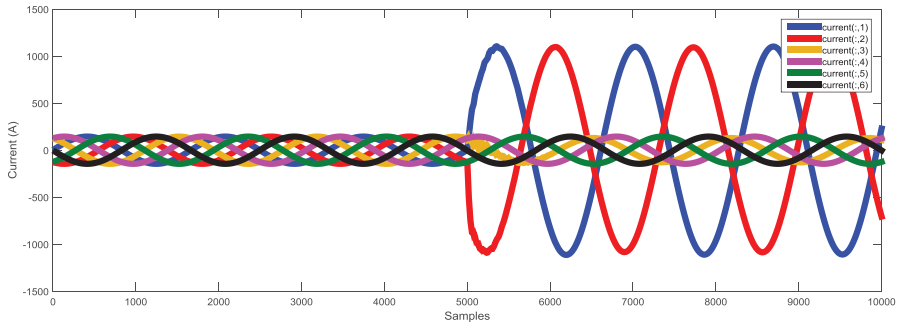

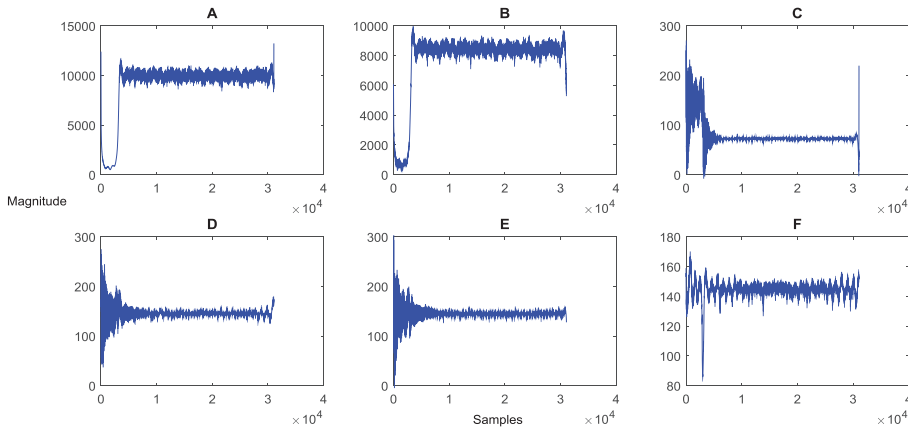Fig. 5. Six phase current during ABG fault at 5 km at FIT=0.05 seconds with R_f = 5 Ω and R_g = 10 Ω

Fig. 6. Hilbert Huang transform coefficients of six phase current during ABG fault at 5 km at FIT=0.05 seconds with R_f = 5 Ω and R_g = 10 Ω

TABLE II

TEST RESULT FOR ABG FAULT AT 5 KM AT FIT = 0.05 SECONDS WITH R_F = 5 Ω AND R_G = 10 Ω

Phase	Hilbert Huang Transform Coefficients
A	1.3184*10^4
B	9.6480*10^3
C	260.7206
D	265.2478
E	293.4751
F	166.8657

B. Performance in Case of BFG Fault: Case-II

The proposed fault detection technique is tested for BFG double line to ground fault when BFG fault is triggered at 20 km away from the relaying point at fault inception time of 0.1 seconds with R_f = 10 Ω and R_g = 15 Ω. Fig. 7 depicts the waveform of six phase current when the six phase transmission line is subjected to BFG fault at 20 km away from the relay location at FIT = 0.1 seconds. The process of feature extraction using Hilbert Huang transform for six phase current during BFG fault is demonstrated in Fig. 8. Fig. 8 depicts the Hilbert Huang transform coefficients of six phase current during

BFG fault. As observed from Fig. 8, the magnitudes of Hilbert Huang coefficients of phase-'B' and 'F' are greater than the magnitudes of Hilbert Huang coefficients of other phases. Table III shows the response of proposed fault detection and classification technique for BFG fault. From the simulation results as shown in Table III, it is clear that the magnitudes of Hilbert Huang coefficients of the faulted phases are greater than the magnitudes of Hilbert Huang coefficients of the healthy phases. Therefore, it is clear from Table III that the BFG fault is correctly identified by the HHT-based relay.
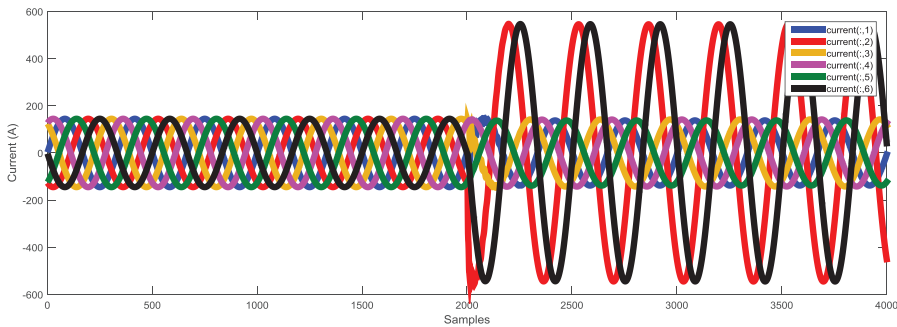

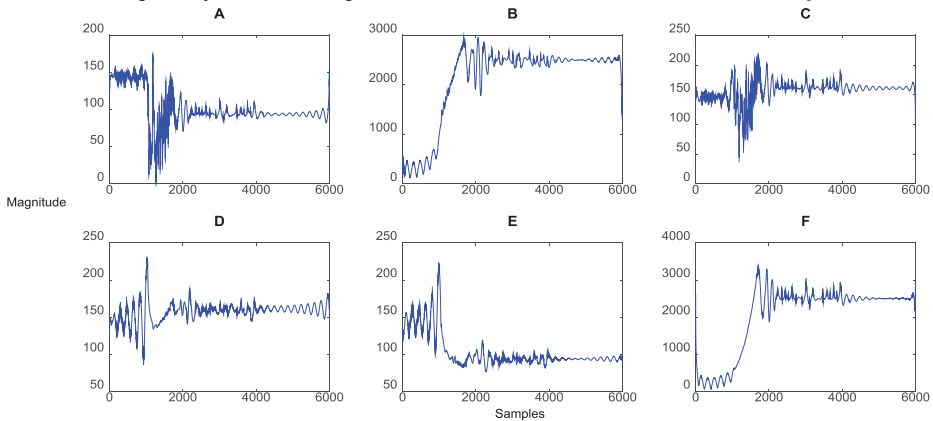Fig. 7. Six phase current during BFG fault at 20 km at FIT=0.1 seconds with R_f = 10 Ω and R_g = 15 Ω

Fig. 8. Hilbert Huang transform coefficients of six phase current during BFG fault at 20 km at FIT=0.1 seconds with R_f = 10 Ω and R_g = 15 Ω

TABLE III

TEST RESULT FOR BFG FAULT AT 20 KM AT FIT = 0.1 SECONDS WITH R_F = 10 Ω AND R_G = 15 Ω

Phase	Hilbert Huang Transform Coefficients
A	171.1185
B	2.9675*10^3
C	213.1655
D	229.3242
E	217.8900
F	3.3120*10^3

C. Performance in Case of CEG Fault: Case-III

Proposed HHT-based relay is tested for CEG double line to ground fault when CEG fault is created at 35 km away from the relay location at fault inception time of 0.15 seconds with R_f = 15 Ω and R_g = 20 Ω. Fig. 9 shows the waveform of six phase current when the six phase transmission line is subjected to CEG fault at 35 km away from the relay location at FIT = 0.15 seconds. The process of feature extraction using Hilbert Huang transform for six phase current during CEG fault is depicted in Fig. 10. Fig. 10 depicts the Hilbert Huang coefficients of six phase current during CEG fault. As

observed from Fig. 10, the magnitudes of Hilbert Huang coefficients of phase-'C' and 'E' are greater than the magnitudes of Hilbert Huang coefficients of other phases. Table IV depicts the response of proposed fault detection technique for CEG fault. From the simulation results as shown in Table IV, it is clear that the magnitudes of Hilbert Huang coefficients of the faulted phases are greater than the magnitudes of Hilbert Huang coefficients of the healthy phases. Therefore, it is clear from Table IV that the CEG fault is correctly detected by the proposed fault detection technique.
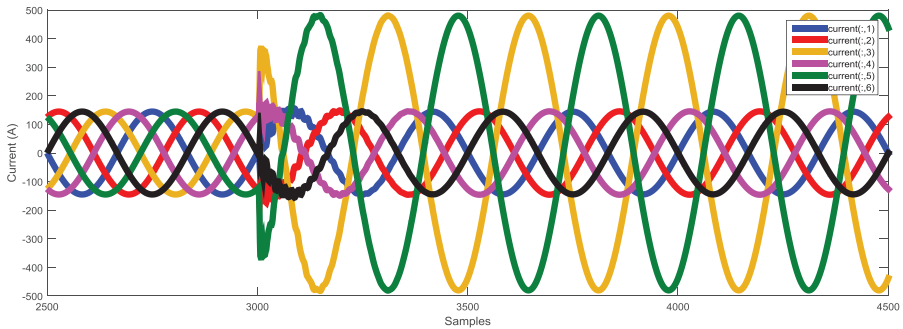

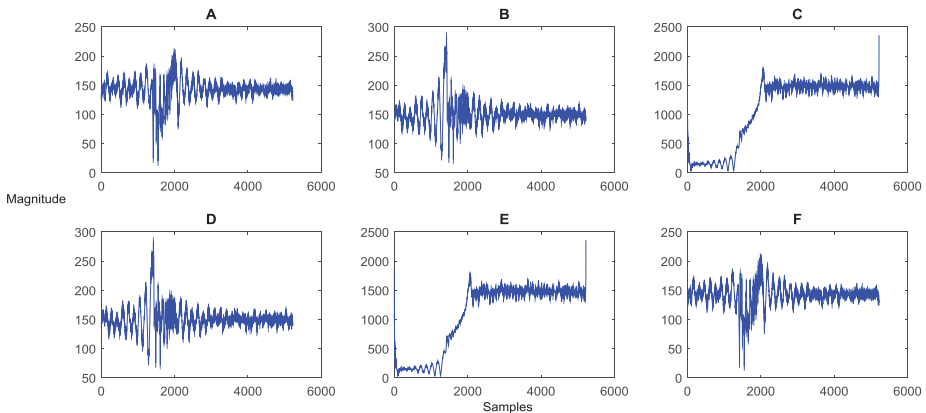Fig. 9. Six phase current during CEG fault at 35 km at FIT=0.15 seconds with R_f = 15 Ω and R_g = 20 Ω

Fig. 10. Hilbert Huang transform coefficients of six phase current during CEG fault at 35 km at FIT=0.15 seconds with R_f = 15 Ω and R_g = 20 Ω

TABLE IV
TEST RESULT FOR CEG FAULT AT 35 KM AT FIT= 0.15 SECONDS WITH R_F = 15 Ω AND R_G = 20 Ω

Phase	Hilbert Huang Transform Coefficients
A	205.3446
B	282.9507
C	2.3483*10^3
D	282.9474
E	2.3481*10^3
F	205.3398

D. Performance in Case of BDG Fault: Case-IV

To investigate the effect of double line to ground BDG fault on the performance of the proposed fault detection technique, a phase BDG fault is created at 50 km away from the relaying point at fault inception time of 0.2 seconds with $R_f = 25$ Ω and $R_g = 30$ Ω. Fig. 11 demonstrates the waveform of six phase current when the six phase transmission line is subjected to BDG fault at 50 km away from the relay location at FIT = 0.2 seconds. Fig. 12 depicts the process of feature extraction using Hilbert Huang transform. Fig. 12 depicts the Hilbert Huang coefficients of six phase current during BDG

fault. As observed from Fig. 12, the magnitudes of Hilbert Huang coefficients of phase- 'B' and 'D' are greater than the magnitudes of Hilbert Huang coefficients of other phases. Table V depicts the test results of proposed fault detection and classification technique for BDG fault. From the simulation results as shown in Table V, it is clear that the magnitudes of Hilbert Huang coefficients of the faulted phases are greater than the magnitudes of Hilbert Huang coefficients of the healthy phases. It is observed from Table V that the BDG fault is correctly identified by the proposed technique.
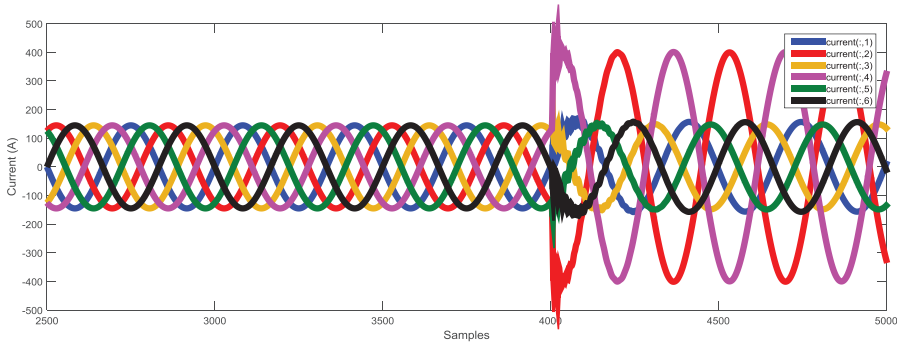

Fig. 11. Six phase current during BDG fault at 50 km at FIT=0.2 seconds with $R_f = 25$ Ω and $R_g = 30$ Ω
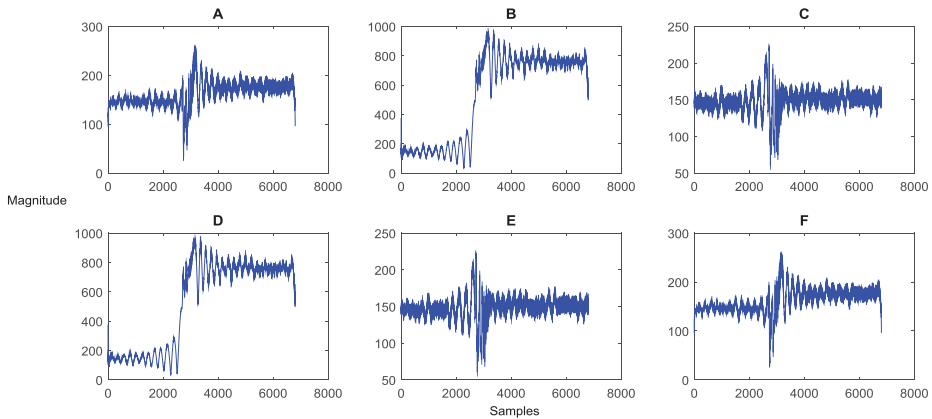

Fig. 12. Hilbert Huang transform coefficients of six phase current during BDG fault at 50 km at FIT=0.2 seconds with $R_f = 25$ Ω and $R_g = 30$ Ω

TABLE V

TEST RESULT FOR BDG FAULT AT 50 KM AT FIT= 0.2 SECONDS WITH $R_F = 25$ Ω AND $R_G = 30$ Ω

Phase	Hilbert Huang Transform Coefficients
A	252.9213
B	957.2747
C	220.3264
D	957.2805
E	220.3286
F	252.9323

E. Performance in Case of AFG Fault: Case-V

The appropriateness of the proposed fault detection technique has been tested by evaluating its performance for AFG double line to ground fault when AFG fault is triggered at 65 km away from the relay location at fault inception time of 0.25 seconds with $R_f = 30\ \Omega$ and $R_g = 35\ \Omega$. Fig. 13 demonstrates the waveform of six phase current when the six phase transmission line is subjected to AFG fault at 65 km away from the relay location at FIT = 0.25 seconds. Fig. 14 demonstrates the procedure of feature extraction using Hilbert Huang transform. Fig. 14 depicts the Hilbert Huang coefficients of six phase

current during AFG fault. As observed from Fig. 14, the magnitudes of Hilbert Huang coefficients of phase-'A' and 'F' are greater than the magnitudes of Hilbert Huang coefficients of other phases. Table VI depicts the response of proposed fault detection/classification technique for AFG fault. From the simulation results as shown in Table VI, it is clear that the magnitudes of Hilbert Huang coefficients of the faulted phases are greater than the magnitudes of Hilbert Huang coefficients of the healthy phases. Therefore, it is clear from Table VI that the proposed technique correctly detects AFG fault.
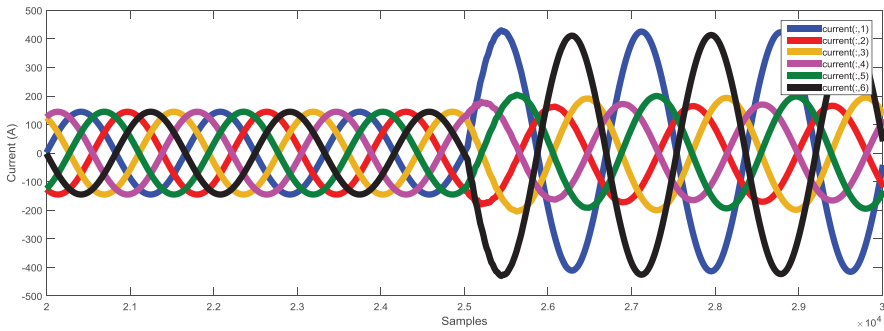

Fig. 13. Six phase current during AFG fault at 65 km at FIT=0.25 seconds with $R_f = 30\ \Omega$ and $R_g = 35\ \Omega$
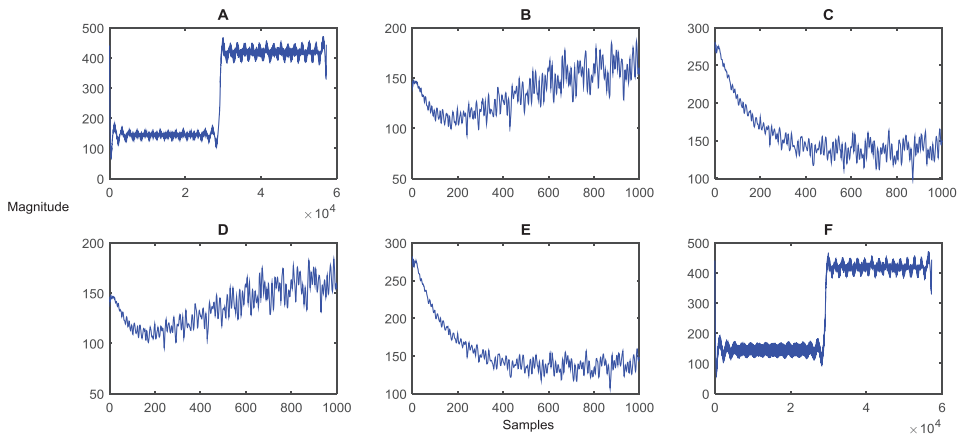

Fig. 14. Hilbert Huang transform coefficients of six phase current during AFG fault at 65 km at FIT=0.25 seconds with $R_f = 30\ \Omega$ and $R_g = 35\ \Omega$

TABLE VI

TEST RESULT FOR AFG FAULT AT 65 KM AT FIT=0.25 SECONDS WITH $R_F = 30\ \Omega$ AND $R_G = 35\ \Omega$

Phase	Hilbert Huang Transform Coefficients
A	456.0421
B	227.5951
C	287.6790
D	218.6629
E	288.3778
F	455.9232

F. Performance in Case of CDG Fault: Case-VI

The response of the proposed fault detection technique has been analyzed for CDG double line to ground fault when CDG fault is created at 60 km away from the relaying point at fault inception time of 0.025 seconds with R_f = 14 Ω and R_g = 18 Ω. Fig. 15 shows the waveform of six phase current when the six phase transmission line is subjected to CDG fault at 60 km away from the relay location at FIT = 0.025 seconds. The process of feature extraction using Hilbert Huang transform for six phase current during CDG fault is depicted in Fig. 16. Fig. 16 depicts the Hilbert Huang

coefficients of six phase current during CDG fault. As observed from Fig. 16, the magnitudes of Hilbert Huang coefficients of phase-'C' and 'D' are greater than the magnitudes of Hilbert Huang coefficients of other phases. Table VII depicts the response of proposed fault detection and classification technique for CDG fault. From the simulation results as shown in Table VII, it is clear that the magnitudes of Hilbert Huang coefficients of the faulted phases are greater than the magnitudes of Hilbert Huang coefficients of the healthy phases. It can be observed from Table VII that the proposed technique correctly detects double line to ground CDG fault.
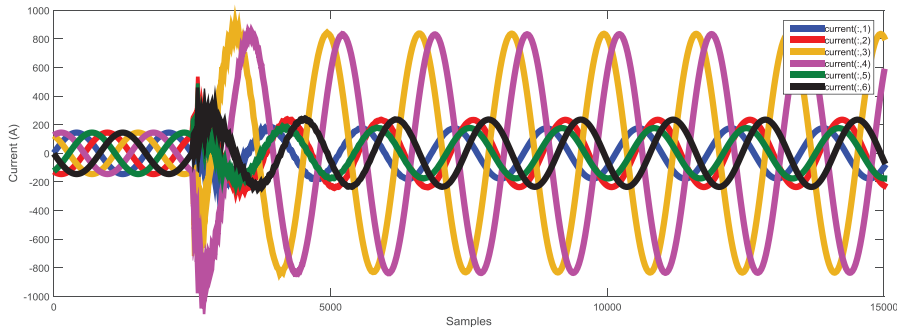

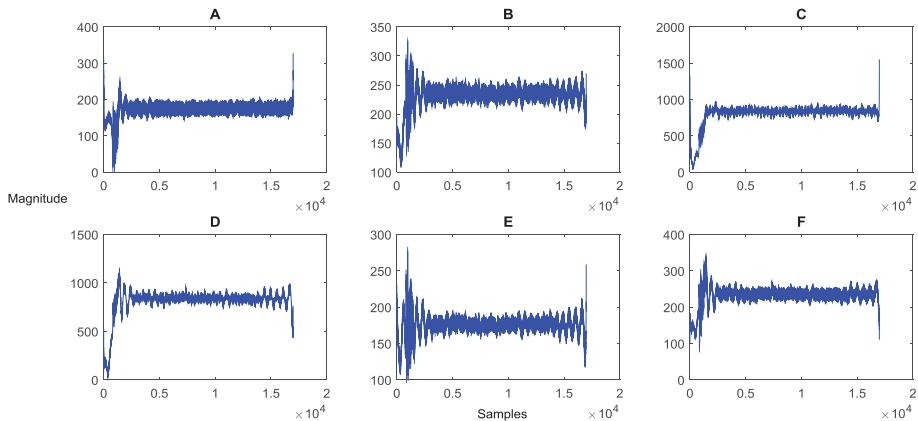Fig. 15. Six phase current during CDG fault at 60 km at FIT=0.025 seconds with R_f= 14 Ω and R_g = 18 Ω

Fig. 16. Hilbert Huang transform coefficients of six phase current during CDG fault at 60 km at FIT=0.025 seconds with R_f = 14 Ω and R_g = 18 Ω

TABLE VII

TEST RESULT FOR CDG FAULT AT 60 KM AT FIT=0.025 SECONDS WITH R_F = 14 Ω AND R_G = 18 Ω

Phase	Hilbert Huang Transform Coefficients
A	326.0328
B	325.6451
C	1.5456*10^3
D	1.1071*10^3
E	276.2881
F	335.9162

G. Performance in Case of BCG Fault: Case-VII

The proposed fault detection technique is tested for BCG double line to ground fault when BCG fault is simulated at 55 km away from the relaying point at fault inception time of 0.075 seconds with R_f = 12 Ω and R_g = 8 Ω. Fig. 17 shows the waveform of six phase current when the six phase transmission line is subjected to BCG fault at 55 km away from the relay location at FIT = 0.075 seconds. The process of feature extraction using Hilbert Huang transform for six phase current during BCG fault has been depicted in Fig. 18. Fig. 18 depicts the Hilbert Huang coefficients of six phase current during

BCG fault. As can be seen from Fig. 18, the magnitudes of Hilbert Huang coefficients of phase-'B' and 'C' are greater than the magnitudes of Hilbert Huang coefficients of other phases. Table VIII reports the response of proposed fault detection and classification technique for BCG fault. From the simulation results as shown in Table VIII, it is clear that the magnitudes of Hilbert Huang coefficients of the faulted phases are greater than the magnitudes of Hilbert Huang coefficients of the healthy phases. It can be concluded from Table VIII that the relay detects BCG fault correctly.
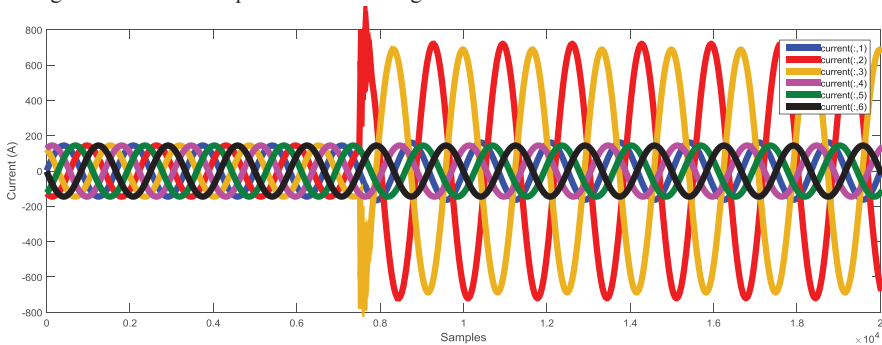

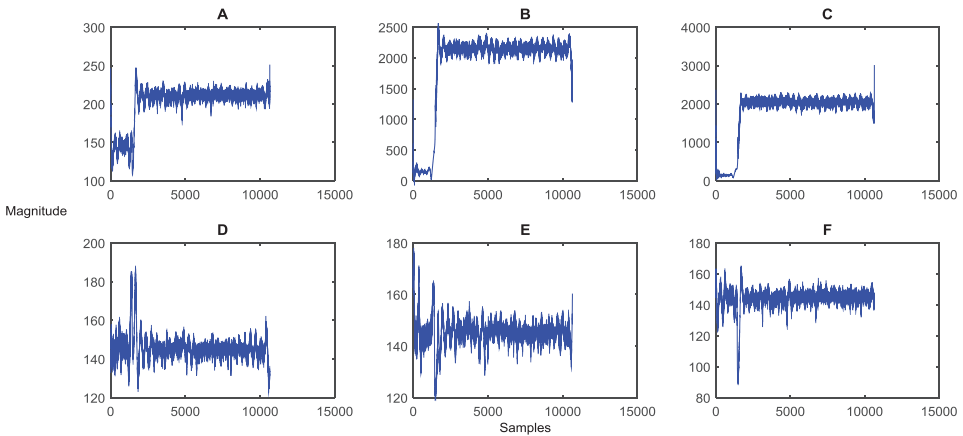Fig. 17. Six phase current during BCG fault at 55 km at FIT=0.075 seconds with R_f = 12 Ω and R_g = 8 Ω

Fig. 18. Hilbert Huang transform coefficients of six phase current during BCG fault at 55 km at FIT=0.075 seconds with R_f = 12 Ω and R_g = 8 Ω

TABLE VIII

TEST RESULT FOR BCG FAULT AT 55 KM AT FIT=0.075 SECONDS WITH R_F = 12 Ω AND R_G = 8 Ω

Phase	Hilbert Huang Transform Coefficients
A	250.6014
B	2.4846*10^3
C	3.0023*10^3
D	185.5797
E	176.0970
F	161.9812

H. Performance in Case of DEG Fault: Case-VIII

The proposed fault detection scheme is tested for DEG double line to ground fault when DEG fault is created at 30 km away from the relaying point at fault inception time of 0.125 seconds with $R_f = 6\ \Omega$ and $R_g = 4\ \Omega$. Fig. 19 demonstrates the waveform of six phase current when the six phase transmission line is subjected to DEG fault at 30 km away from the relay location at FIT = 0125 seconds. The process of feature extraction using Hilbert Huang transform for six phase current during DEG fault is depicted in Fig. 20. Fig. 20 depicts the Hilbert Huang coefficients of six phase current during DEG fault. As

can be seen from Fig. 20, the magnitudes of Hilbert Huang coefficients of phase-'D' and 'E' are greater than the magnitudes of Hilbert Huang coefficients of other phases. Table IX reports the response of proposed fault detection and classification technique for DEG fault. From the simulation results as reported in Table IX, it is observed that the magnitudes of Hilbert Huang coefficients of the faulted phases are greater than the magnitudes of Hilbert Huang coefficients of the healthy phases. From Table IX, it is clear that the DEG fault is correctly detected by the proposed fault detection technique.
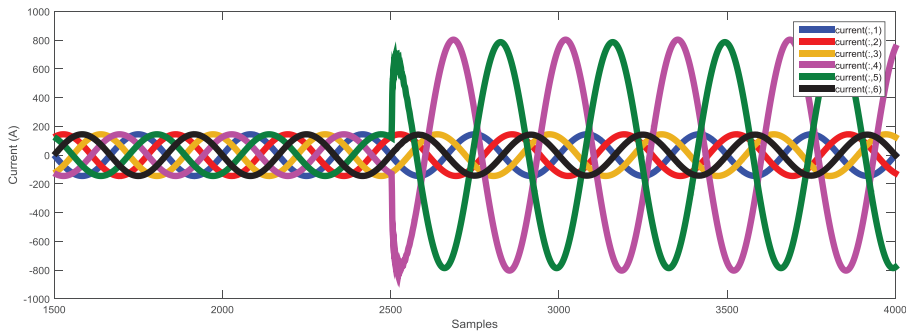

Fig. 19. Six phase current during DEG fault at 30 km at FIT=0.125 seconds with $R_f = 6\ \Omega$ and $R_g = 4\ \Omega$
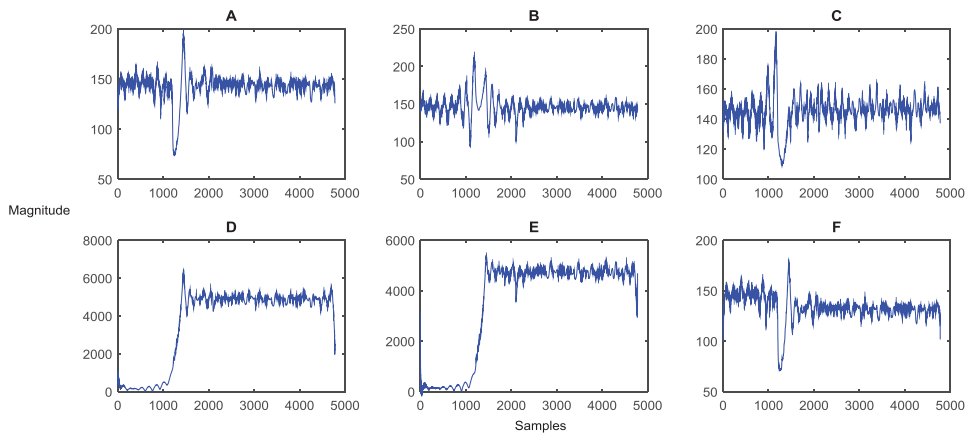

Fig. 20. Hilbert Huang transform coefficients of six phase current during DEG fault at 30 km at FIT=0.125 seconds with $R_f = 6\ \Omega$ and $R_g = 4\ \Omega$

TABLE IX

TEST RESULT FOR DEG FAULT AT 30 KM AT FIT=0.125 SECONDS WITH $R_F = 6\ \Omega$ AND $R_G = 4\ \Omega$

Phase	Hilbert Huang Transform Coefficients
A	194.8826
B	212.7786
C	194.9312
D	6.2882*10^3
E	5.3144*10^3
F	177.9366

I. Performance in Case of EFG Fault: Case-IX

The fault detection and faulty phase identification technique is checked for EFG double line to ground fault when EFG fault is triggered at 25 km away from the relaying point at fault inception time of 0.175 seconds with $R_f = 2\ \Omega$ and $R_g = 1\ \Omega$. Fig. 21 depicts the waveform of six phase current when the six phase transmission line is subjected to EFG fault at 25 km away from the relay location at FIT = 0.175 seconds. The process of feature extraction using Hilbert Huang transform for six phase current during EFG fault is shown in Fig. 22. Fig. 22 depicts the Hilbert Huang coefficients of six phase

current during EFG fault. As can be seen from Fig. 22, the magnitudes of Hilbert Huang coefficients of phase-'E' and 'F' are greater than the magnitudes of Hilbert Huang coefficients of other phases. Table X shows the response of proposed fault detection and classification technique for EFG fault. From the test results as depicted in Table X, it is clear that the magnitudes of Hilbert Huang coefficients of the faulted phases are greater than the magnitudes of Hilbert Huang coefficients of the healthy phases. It is noticeably observed from Table X that the relay detects the EFG fault correctly.
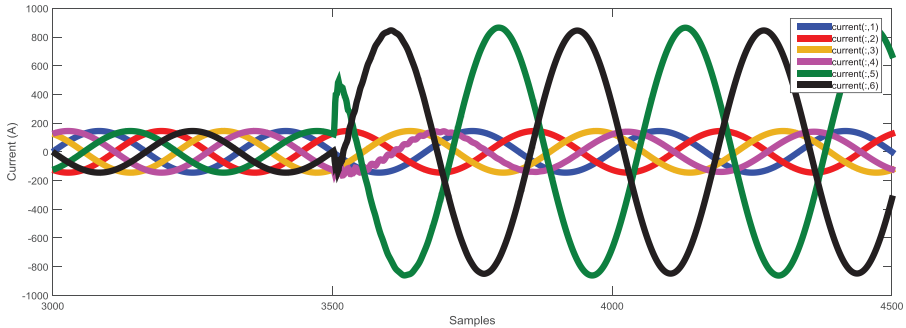

Fig. 21. Six phase current during EFG fault at 25 km at FIT=0.175 seconds with $R_f = 2\ \Omega$ and $R_g = 1\ \Omega$
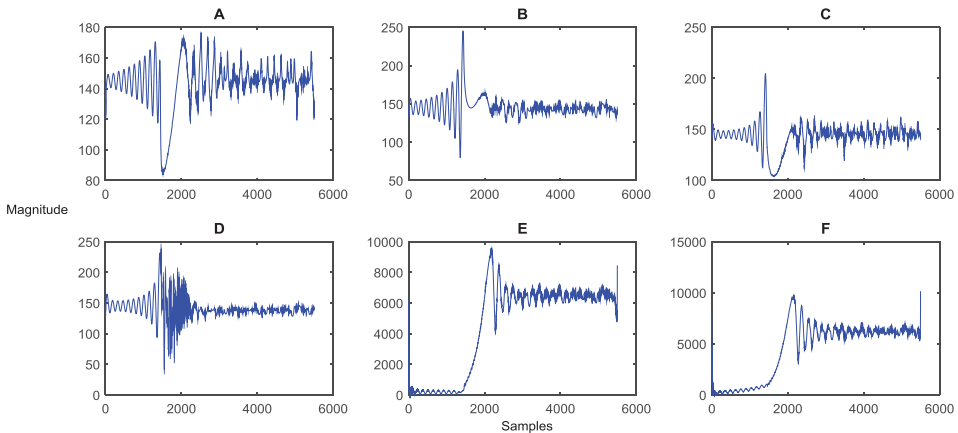

Fig. 22. Hilbert Huang transform coefficients of six phase current during EFG fault at 25 km at FIT=0.175 seconds with $R_f = 2\ \Omega$ and $R_g = 1\ \Omega$

TABLE X
TEST RESULT FOR EFG FAULT AT 25 KM AT FIT=0.175 SECONDS WITH $R_F = 2\ \Omega$ AND $R_G = 1\ \Omega$

Phase	Hilbert Huang Transform Coefficients
A	176.4939
B	245.0442
C	204.5428
D	238.5428
E	9.5278×10^3
F	1.0094×10^4

J. Performance in Case of ADG Fault: Case-X

The response of the proposed technique has been analyzed for ADG double line to ground fault when ADG fault triggered at 10 km away from the relaying point at fault inception time of 0.225 seconds with $R_f = 8\ \Omega$ and $R_g = 16\ \Omega$. Fig. 23 shows the waveform of six phase current when the six phase transmission line is subjected to ADG fault at 10 km away from the relaying point at FIT = 0.225 seconds. The procedure of feature extraction using Hilbert Huang transform for six phase current during ADG fault is depicted in Fig. 24. Fig. 24 shows the Hilbert Huang coefficients of six phase current during

ADG fault. As can be seen from Fig. 24, the magnitudes of Hilbert Huang coefficients of phase-'A' and 'D' are greater than the magnitudes of Hilbert Huang coefficients of other phases. Table XI reports the response of proposed fault detection and classification technique for ADG fault. From the results as shown in Table XI, it is clear that the magnitudes of Hilbert Huang coefficients of the faulted phases are greater than the magnitudes of Hilbert Huang coefficients of the healthy phases. It is clear from Table XI that the ADG fault is correctly identified by the proposed fault detection scheme.
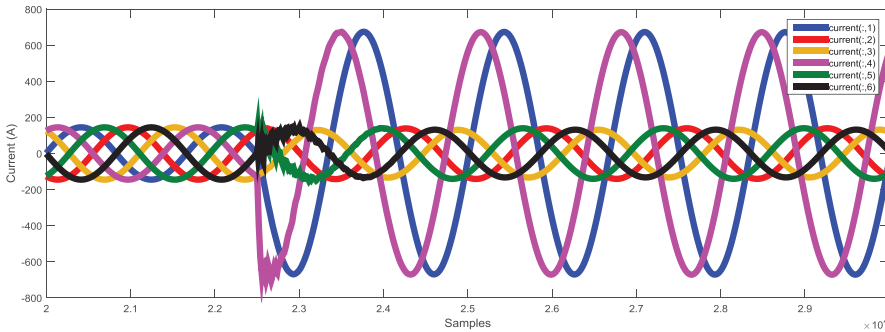

Fig. 23. Six phase current during ADG fault at 10 km at FIT=0.225 seconds with $R_f = 8\ \Omega$ and $R_g = 16\ \Omega$
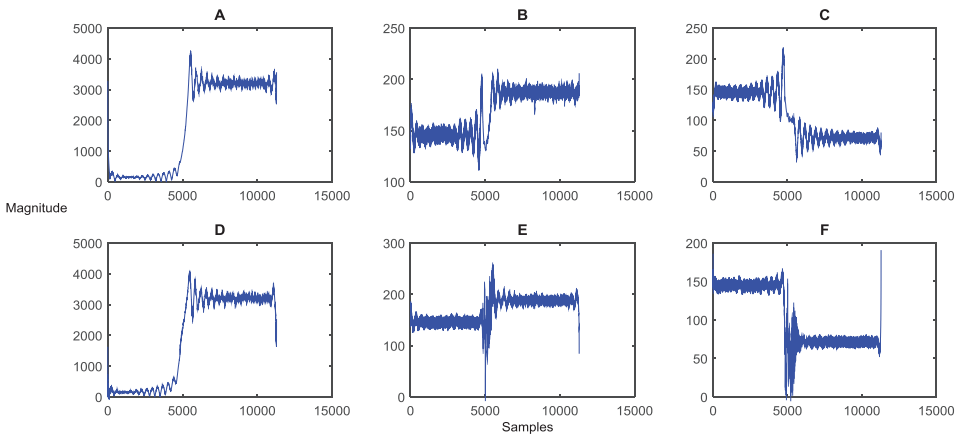

Fig. 24. Hilbert Huang transform coefficients of six phase current during ADG fault at 10 km at FIT=0.225 seconds with $R_f = 8\ \Omega$ and $R_g = 16\ \Omega$

TABLE XI

TEST RESULT FOR ADG FAULT AT 10 KM AT FIT=0.225 SECONDS WITH $R_F = 8\ \Omega$ AND $R_G = 16\ \Omega$

Phase	Hilbert Huang Transform Coefficients
A	$4.1146*10^3$
B	205.4306
C	210.3117
D	$4.0294*10^3$
E	252.1842
F	190.0547

V.   Conclusion

This paper proposes a single-ended Hilbert Huang transform (HHT) based double line to ground fault detection and faulty phase identification technique for a 138 kV, 60 Hz six phase transmission line. HHT is applied to the six phase currents recorded at bus-1 of the six phase transmission line. The Hilbert Huang transform coefficients of six phase currents are used for fault detection and faulty phase identification. The performance of the proposed technique is studied for the following situations: fault type, fault location, fault inception time, fault resistance and ground resistance. According to the test results, the proposed technique is able to detect the double line to ground faults and identify the faulty phase correctly.

References

[1] G. Kapoor, Six phase transmission line boundary protection using wavelet transform, *Proceedings of the 8ᵗʰ IEEE India International Conference on Power Electronics (IICPE)*, December 13-15, Jaipur, India, 2018.

[2] G. Kapoor, Fault detection of phase to phase fault in series capacitor compensated six phase transmission line using wavelet transform, *Jordan Journal of Electrical Engineering, vol. 4*(3), pp. 151-164, 2018.

[3] G. Kapoor, Six phase transmission line boundary protection using mathematical morphology, *Proceedings of the IEEE International Conference on Computing, Power and Communication Technologies (GUCON)*, pp. 857-861, Greater Noida, India, September 28-29, 2018.

[4] G. Kapoor, Detection of phase to phase faults and identification of faulty phases in series capacitor compensated six phase transmission line using the norm of wavelet transform, *I-Managers Journal of Digital Signal Processing, vol. 6* (1), pp. 10-20, 2018.

[5] S. N. Ananthan, R. Padmanabhan, R. Meyur, B. Mallikarjuna, M. J. B. Reddy, and D. K. Mohanta, Real-time fault analysis of transmission lines using wavelet multi-resolution analysis based frequency-domain approach, *IET Science, Measurement and Technology, vol. 10* (7), pp. 693-703, 2016.

[6] U. J. Patel, N. G. Chothani, and P. J. Bhatt, Sequence-space-aided SVM classifier for disturbance detection in series compensated transmission line, *IET Science, Measurement and Technology, vol. 12* (8), pp. 983-993, 2018.

[7] A. S. Gomes, M. A. Costa, T. G. A. Faria, and W. M. Caminhas, Detection and Classification of Faults in Power Transmission Lines Using Functional Analysis and Computational Intelligence, *IEEE Transactions on Power Delivery*, vol. 28 (3), pp. 1402-1413, 2013.

[8] M. M. Taheri, H. Seyedi, M. Nojavan, M. Khoshbouy, and B. M. Ivatloo, High Speed Decision Tree- Based Series Compensated Transmission Lines Protection Using Differential Phase Angle of Superimposed Current, *IEEE Transactions on Power Delivery*, *vol. 33* (6), pp. 3130-3138, 2018.

[9] D. Kumar and P. S. Bhowmik, Artificial neural network and phasor data based islanding detection in smart grid, *IET Generation, Transmission and Distribution*, *vol. 12* (21), pp. 5843-5850, 2018.

[10] W. Leterme, S. P. Azad, and D. V. Hertem, HVDC grid protection algorithm design in phase and modal domains, *IET Renewable Power Generation*, *vol. 12* (13), pp. 1538-1546, 2018.

[11] A. Saber, A. Emam, and H. Elghazaly, A backup Protection Technique for Three-Terminal Multisection Compound Transmission Lines, *IEEE Transactions on Smart Grid*, *vol. 9* (6), pp. 5653-5663, 2018.

[12] M. D. Shafiullah and M. A. Abido, S-Transform Based FFNN Approach for Distribution Grids Fault Detection and Classification, *IEEE Access*, *vol. 6*, pp. 8080-8088, 2018.

[13] S. K. Shukla, E. Koley, and S. Ghosh, DC offset estimation-based fault detection in transmission line during power swing using ensemble of decision tree, *IET Science, Measurement and Technology*, *vol. 13* (2), pp. 212-222, 2019.

[14] Q. Wan and L. Zhao, A novel fault section location method for small current grounding fault based on Hilbert Huang transform with wavelet packet transform preprocessing, *Proceedings of the 11ᵗʰ IEEE International Conference on Intelligent Computational Technology and Automation (ICICTA)*, pp. 365-370, Changsha, China, 2018.

[15] G. Kapoor, A contemporary discrete wavelet transform based twelve phase series capacitor compensated transmission line protection, *International Journal of Engineering, Research and Technology, vol. 7*(5), pp. 263-271, 2018.